Progress In Electromagnetics Research, Vol. 148, 113–128, 2014

Lattice Maxwell's Equations

Fernando L. Teixeira*

(*Invited Paper*)

Abstract—We discuss the *ab initio* rendering of four-dimensional (4-d) spacetime of Maxwell's equations on random (irregular) lattices. This rendering is based on casting Maxwell's equations in the framework of the exterior calculus of differential forms, and a translation thereof to a simplicial complex whereby fields and causative sources are represented as differential p-forms and paired with the oriented p-dimensional geometrical objects that comprise the set of spacetime lattice cells (simplices). We pay particular attention to the case of simplicial spacetime lattices because these can serve as building blocks of lattices made of more generic cells (polygons). The generalized Stokes' theorem is used to construct discrete calculus operations on the lattice based upon combinatorial relations depending solely on the connectivity and relative orientation among simplices. This rendering provides a natural factorization of (lattice) 4-d spacetime Maxwell's equations into a metric-free part and a metric-dependent part. The latter is encoded by discrete Hodge star operators which are built using Whitney forms, i.e., canonical interpolants for discrete differential forms. The derivation of Whitney forms is illustrated here using a geometrical construction based on the concept of barycentric coordinates to represent a point on a simplex, and the generalization thereof to represent higher-dimensional objects (lines, areas, volumes, and hypervolumes) in 4-d. We stress the role of the primal lattice, the barycentric dual lattice, and the barycentric decomposition lattice in achieving a complete description of the lattice theory. Lattice Maxwell's equations based on the exterior calculus of differential forms and on the use of Whitney forms as field interpolants inherits the symplectic structure and discrete analogues of conservation laws present in the continuum theory, such as energy and charge conservation. It also provides precise localization rules for the degrees of freedom associated with the different fields and sources on the lattice, and design principles for constructing consistent numerical solution methods that are free from spurious modes, spectral pollution, and (unconditional) numerical instabilities. We also briefly consider the relationship between lattice 4-d Maxwell's equations and some incarnations of discretization schemes for Maxwell's equations in $(3+1)$-d, such as finite-differences and finite-elements.

1. INTRODUCTION AND MOTIVATION

The need for discretization of field equations arises in many areas. The discretization allows for numerical computation of (often approximate) field solutions in non-perturbative regimes and on complex domains with non-trivial boundary and/or initial conditions. The discretization of Maxwell's equations invariably causes changes on the properties of the field solutions ("numerical artifacts"). Some of these changes are unavoidable, such as the appearance of a finite cut-off frequency, the breaking of translational and rotational symmetries (although some discrete symmetries may still remain due to the periodicity of the lattice), aliasing, and the presence of grid-dispersion ("numerical dispersion") effects. Nevertheless,

Received 29 June 2014, Accepted 19 July 2014, Scheduled 21 July 2014
Invited paper for the Commemorative Collection on the 150-Year Anniversary of Maxwell's Equations.
* Corresponding author: Fernando Lisboa Teixeira (teixeira.5@osu.edu).
The author is with the ElectroScience Laboratory, Department of Electrical and Computer Engineering, the Ohio State University, 1330 Kinnear Road, Columbus, Ohio 43212-1166, USA.

these types of artifacts are *controllable* in the sense that they can be made arbitrarily small by employing progressively smaller lattice elements (i.e., additional degrees of freedom).

Associated to many discretization schemes, however, there are other more deleterious types of numerical artifacts stemming from the violation of conservation laws such as momentum, energy, charge, and symmetries such as time-reversal invariance, among others[†]. Examples of such type of numerical artifacts are unconditional instabilities and/or artificial dissipation (in time-marching schemes) and spectral pollution through the emergence of spurious modes. If present, these latter types of numerical artifacts are more difficult (or even unfeasible) to control.

A basic motivation behind the *ab initio* derivation of lattice Maxwell's equations stems from the need to obtain a consistent representation of electromagnetic fields on irregular lattices, whereby conservation laws and other basic theorems of the continuum theory are automatically preserved and only the first type (controllable) of approximation artifacts, as alluded above, are present. To provide sufficient generality, it is desirable to achieve consistency independently from the metric properties of the lattice (i.e., from the geometrical shapes of the individual lattice cells), as the latter can vary across lattice instantiations according to the intended application(s). Another, secondary motivation is to confine the source of the approximation artifacts to a minimum number of discretization steps. Finally, the *ab initio* derivation of Maxwell's equations also provides a route for the identification and systematic classification of potential sources of inconsistency arising in commonly employed discretization methods such as finite elements, finite differences, and finite elements.

2. FUNDAMENTALS

The action for the electromagnetic field in a four-dimensional (4-d) spacetime domain Ω_4 with flat metric is given by the integral [1–4]

$$\mathcal{S}[A,\mathcal{J}] = \int_{\Omega_4} \mathcal{L} = \int_{\Omega_4} \left(\frac{1}{2} F \wedge *F - A \wedge *\mathcal{J} \right) \tag{1}$$

where $\mathcal{L}$ is the Lagrangian 4-form, $F = \mathrm{d}A$ the Faraday 2-form, A the potential 1-form, $*\mathcal{J}$ the charge-current density 3-form, $\wedge$ the (anti-commutative) exterior product, and d the 4-d exterior derivative [6]. The Hodge star operator $*$ [5–7] is a metric-dependent map (isomorphism) from p-forms to $(n-p)$-forms, $p = 0, \ldots, n$ (here, $n = 4$). By letting a denote a small variation on A, using integration by parts, and ignoring second-order terms in a, one obtains

$$\delta\mathcal{S} = \mathcal{S}[A+a,\mathcal{J}] - \mathcal{S}[A,\mathcal{J}] = \int_{\Omega_4} da \wedge *dA - \int_{\Omega^4} a \wedge *\mathcal{J} = \int_{\Omega_4} a \wedge (d * dA - *\mathcal{J}) \tag{2}$$

so that, upon enforcing the stationary principle $\delta\mathcal{S} = 0$ in the classical case, the following Euler-Lagrange equation results

$$\mathrm{d}G = *\mathcal{J} \tag{3}$$

where G is the Maxwell 2-form, $G = *F$ [1, 5, 6, 8, 9]. In addition, since $\mathrm{d}^2 = 0$, the relation $F = \mathrm{d}A$ implies

$$\mathrm{d}F = 0 \tag{4}$$

Taken together, (3) and (4) constitute Maxwell's equations in 4-d [6, 8–11]. Apart from its very compact form, these relations show two salient features [5, 6]. First, they naturally split into a metric-dependent part (3) and a purely topological (i.e., metric-free or manifestly invariant under diffeomorphisms) part (4). This is because d is a metric-free operator [12] and, as such, only (3) is modified under a change on the metric (as encoded by the $*$ operator), whereas (4) remains invariant. The second feature is that (3) and (4) can be *exactly* transcribed onto a irregular lattice because both d and $*$ operators admit well-defined, direct counterpart representations on such lattices. We will discuss below these observations in detail, and work out some of their practical consequences.

[†] Note that, oftentimes, conservation laws can be preserved at the discrete level upon a suitable redefinition of the conserved quantities. The lack of conservation alluded here is w.r.t. any appropriate redefinition of "conserved" quantities. Also, recall that, from Noether's theorem, conservation laws are a consequence of underlying symmetries, i.e., violations of the former are due to the breaking of the latter. For example, violation of energy/momentum conservation is caused by lack of invariance under time/space translations.

For notational simplicity, the wedge symbol $\wedge$ will be at times suppressed in what follows when its presence is clear from the context; thus, e.g., $\mathrm{d}x \wedge \mathrm{d}y \to \mathrm{d}x\mathrm{d}y = -\mathrm{d}y\mathrm{d}x$.

3. DIFFERENTIAL FORMS ON A LATTICE

3.1. Primal, Dual, and Decomposition Lattices

Some of the definitions used in [13] are generalized here from 3-d to 4-d, with some slight changes in notation. Given a set of affine points u_0, u_1, ..., u_p, $p = 0, \ldots, 4$ in 4-d spacetime, a p-simplex σ_p is

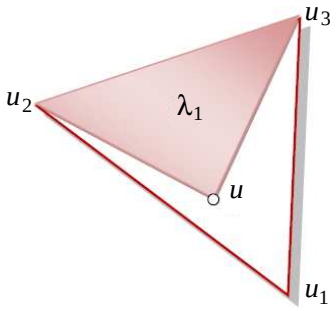

Figure 1. Geometrical construction for the barycentric coordinate λ_1 of a point u in a 2-simplex. The value λ_1 is equal to the ratio between the area indicated in red and the total area of the 2-simplex. An analogous construction can be used in any p-simplex.

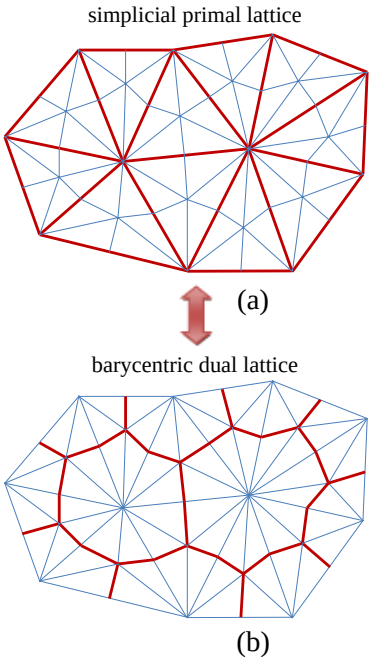

Figure 2. Depiction of a 2-d primal/dual lattice construction. Edges indicated in red color constitute (a) the primal lattice and (b) the barycentric dual lattice. Note that the primal lattice is simplicial but the dual lattice is not so. Note also that individual edges of the dual lattice are not straight, but are composed of two straight segments. The barycentric decomposition lattice underlies these two lattices, with its remaining set of edges indicated in blue color. The barycentric decomposition mesh is sill a simplicial mesh, and is symmetric under permutation of primal lattice nodes. The above construction can be generalized to any number of dimensions.

the region spanned by $u = \sum_{i=0}^{p} \lambda_i u_i$ for all possible values of $\lambda_i \in [0, 1]$, where λ_i is the *barycentric* coordinate associated with u_i such that $\sum_{i=0}^{p} \lambda_i = 1$. Fig. 1 shows, using the 2-d case as example, the geometrical construction of the barycentric coordinate λ_1 associated to a point u within a 2-simplex (triangle). In this case, the value of λ_1 is simply the ratio between the areas of the triangles defined by $[u, u_2, u_3]$ and by $[u_1, u_2, u_3]$. A similar construction can be made for a general p-simplex. A 0-simplex is simply a point, a 1-simplex is an edge (line segment), a 2-simplex is a face or plaquette (triangle), a 3-simplex is an elementary volume (tetrahedron), and a 4-simplex is an elementary hypervolume (penthachoron). For convenience, we may denote $\sigma_p = [u_0, u_1, \ldots, u_p]$. Note that an oriented p-simplex changes sign under an orientation reversal, so that, for example $[u_1, u_2, u_3] = [u_3, u_1, u_2] = -[u_2, u_1, u_3]$.

A simplicial complex in 4-d corresponds to a set of simplices of $p = 0, \ldots, 4$ degrees comprising an irregular (in general) tessellation of spacetime, i.e., where the boundaries of each p-simplex comprise a set of lower dimensional, $(p-1)$-simplices, for $p = 1, \ldots, 4$ (that is, with no overlaps or gaps). We identify such simplicial complex as the *primal* lattice. Associated to any primal lattice, two other affine invariant lattice constructions of interest exist, viz. the *barycentric dual* lattice and the *barycentric decomposition* lattice, as illustrated in Fig. 2. In what follows, p-cells of the dual lattice are denoted as $\tilde{\sigma}_p$. Note that we use the terminology *cell* in this case (rather than simplex) due to their more general shape (polygons). Likewise, the dual lattice constitutes a cell complex. In a n-d domain, p-dimensional cells of the barycentric dual lattice are in a bijective correspondence with $(n-p)$-simplices of the primal lattice. i.e., they form a isomorphism $\{\tilde{\sigma}_p\} \cong \{\sigma_{n-p}\}$. As discussed in detail elsewhere [5, 14], the primal and dual lattices exhibit different *types* of orientation: the primal lattice is typically chosen as having *inner* orientation and the dual lattice as having *outer* orientation. These two types of orientation exhibit different behavior under reflection, a distinction akin to that between proper (or polar) tensors and pseudo (or axial) tensors for example. As evident from Fig. 2, every cell of both the primal and barycentric dual lattices can be assembled from a set of simplices of the barycentric decomposition lattice. In addition, the barycentric decomposition lattice is simplicial even though the barycentric dual lattice is not.

3.2. Localization of Degrees-of-Freedom

A differential p-form $\alpha^{(p)}$ can be thought of as a p-dimensional oriented density so that its integral over each oriented p-cell (simplex) σ_p of the (simplicial) lattice written as

$$\int_{\sigma_p} \alpha^{(p)} \tag{5}$$

is well defined and yields a scalar value as a result. Differential forms thus provide precise assignment rules, according to their degree, for the localization of the degree-of-freedom (DoF) of the lattice field theory: a p-form is always assigned to a p-cell. In particular, the DoFs of the 2-forms G in (3) and F in (4) are associated with *face* elements of the lattice, whereas the DoFs of the potential A are associated with *edges* thereof. However, because these forms have different types of orientations: F and A are 'ordinary' differential forms with inner orientation whereas G (as well as $*\mathcal{J}$) is a 'twisted' differential form with outer-orientation [5, 14], they are associated with either the primal (F and A) or the dual lattice (G and $*\mathcal{J}$) discussed above. The connection between fields on the two (primal and dual) lattices is effected through Hodge dualities such as $F = *G$. The need for a primal/dual lattice construction can be also motivated on purely combinatorial [16, 17] or computational [18, 19] grounds as well. In particular, the importance of a dual lattice for a proper definition of the discrete Hodge star operator in the context of field theories and for correctly reproducing topological invariants in the discrete setting was first recognized in [16].

It should also be pointed out that the quantities expressed by (5) are the true *measurable* quantities of the theory (i.e., the fields themselves are not) [14]. Clearly, for the notion of 'measurement' to be a reliable one, the values of the integrals (5) should be continuous with respect to small perturbations on σ_p. Because of this, in the 3-d case for example, 0-forms (evaluated at a point) exhibit full continuity (associated to scalar potential fields), 1-forms exhibit tangential continuity (associated to "intensity" vector fields), 2-forms exhibit surface normal continuity (associated to "flux" vector fields), and 3-forms may exhibit stepwise discontinuities (e.g., scalar charge densities).

4. EXTERIOR DERIVATIVE ON A LATTICE

In order to proceed further, it is necessary first to translate the two operators d and $*$, that appear in (3) and (4), to the lattice setting. The lattice translation of the discrete exterior derivative d is based on the Generalized Stokes' Theorem (GST) [5, 15]. As its name suggests, the GST encompasses the Fundamental Theorem of Calculus in 1-d, Stokes' Theorem in 2-d, and Gauss' Theorem in 3-d, and is valid for any number of dimensions. The GST writes as

$$\int_{\gamma_p} \mathrm{d}\alpha^{(p-1)} = \int_{\partial\gamma_p} \alpha^{(p-1)} \tag{6}$$

for $p = 1, 2, \ldots$. Here, γ_p is an arbitrary p-dimensional domain, ∂ the boundary operator, and $\alpha^{(p-1)}$ a generic $(p-1)$-form. The operator ∂ carries its ordinary meaning [20] as illustrated in Fig. 3, and on a lattice it maps any p-simplex to the set of $(p-1)$-simplices comprising its geometrical boundary. Also illustrated in Fig. 3, one always has $\partial^2 = 0$ (i.e., the 'boundary of a boundary is zero' [21]).

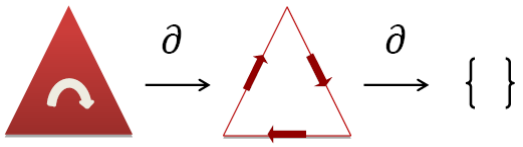

Figure 3. Boundary operator acting on a 2-simplex (oriented triangular cell) and its boundary (three oriented edges). Note the inherited orientation of the boundary 1-simplices. The nilpotency $\partial^2 = 0$ is also illustrated, as the boundary of the union of the 1-simplices shown (a closed loop) is null.

In the continuum, there are no restrictions on the choice of the region of integration γ_p. On the lattice, the GST remains valid except for the fact that γ_p now necessarily comprises the union of some number of p-simplices. For example, for $p = 2$, γ_p corresponds to a union of two-dimensional facets (plaquettes). For any two $\sigma_{p,i}$ and $\sigma_{p,j}$ with $i, j = 1, \ldots, N_p$, where N_p in the number of p-simplices on the lattice, one has

$$\int_{\sigma_{p,i}} \alpha^{(p)} + \int_{\sigma_{p,j}} \alpha^{(p)} = \int_{(\sigma_{p,i}+\sigma_{p,j})} \alpha^{(p)}. \tag{7}$$

so that one can represent γ_p as the formal sum ('chain'), $\gamma_p = \sum_i a_i \sigma_{p,i}$, with some integer coefficients a_i. This means that, for an arbitrary chain γ_p, the evaluation of the integral

$$\int_{\gamma_p} \alpha^{(p)} = \int_{\left(\sum_i a_i \sigma_{p,i}\right)} \alpha^{(p)} = \sum_i a_i \int_{\sigma_{p,i}} \alpha^{(p)} \tag{8}$$

hinges upon the knowledge of the integrals

$$\alpha_i^{(p)} \equiv \int_{\sigma_{p,i}} \alpha^{(p)} \tag{9}$$

for all p-simplices $\sigma_{p,i}$ that comprise the lattice. For some p-form $\alpha^{(p)}$, we call (9) the *contractions* of $\alpha^{(p)}$ with the lattice elements [5]. Such contractions represent the discrete degrees of freedom of the lattice field theory.

Going back to the GST, since $\partial\gamma_p$ is a $(p-1)$-dimensional object on the lattice, we can represent it in terms of $(p-1)$-simplices. In other words, for any $\gamma_{p,i}$, we have

$$\partial\gamma_{p,i} = \partial\left(\sum_i a_i \sigma_{p,i}\right) = \sum_i a_i\, \partial\sigma_{p,i} = \sum_i a_i \sum_j C_{ij}^{(p)} \sigma_{p-1,j} \tag{10}$$

with $i = 1, \ldots, N_p$ and where $C_{ij}^{(p)}$ are elements of the *incidence operators* (matrices) [22], which map any p-simplex $\sigma_{p,j}$ to the $(p-1)$-simplices that comprise its boundary. The entries $C_{i,j}^{(p)}$ assume 0, $+1$, -1

values, with the sign depending on the relative orientation chosen for the individual simplices i and j. This is a consequence of the fact that $C_{i,j}^{(p)}$ represent a purely topological operator (as d) that does not depend on the background metric. On a 4-d lattice, the set of four incidence operators $p = 1, \ldots, 4$ fully encode the connectivity information among the elements of the lattice. It should be clear that an analogous set of operators exists for the dual lattice, which are denoted here as $\tilde{C}_{i,j}^{(p)}$.

Combining (6) and (10), we obtain

$$\int_{\sigma_{p,i}} \mathrm{d}\alpha^{(p-1)} = \int_{\partial\sigma_{p,i}} \alpha^{(p-1)} = \int_{\left(\sum_j C_{ij}^{(p)}\sigma_{p-1,j}\right)} \alpha^{(p-1)} = \sum_j C_{ij}^{(p)} \int_{\sigma_{p-1,j}} \alpha^{(p-1)} \tag{11}$$

or, in terms of the shorthand notation introduced in (9),

$$\left(\mathrm{d}\alpha^{(p-1)}\right)_i = (\mathrm{d}\alpha)_i^{(p)} = \sum_j C_{ij}^{(p)} \alpha_j^{(p-1)}. \tag{12}$$

This last equation is the desired discrete representation of d on a lattice, fully encoded by the incidence operators. Note that, from (6), we have

$$\int_{\gamma_p} \mathrm{d}^2\alpha^{(p-2)} = \int_{\partial\gamma_p} \mathrm{d}\alpha^{(p-2)} = \int_{\partial^2\gamma_p} \alpha^{(p-1)} = 0, \tag{13}$$

where the last equality follows directly from $\partial^2 = 0$. In other words, since (6) implies that ∂ and d are formal adjoint operators, the identity $\partial^2 = 0$ implies $\mathrm{d}^2 = 0$. In turn, this implies the structural constraint[‡]

$$\sum_k C_{ik}^{(p+1)} C_{kj}^{(p)} = 0 \tag{14}$$

and an equivalent one on the dual lattice, i.e.,

$$\sum_k \tilde{C}_{ik}^{(p+1)} \tilde{C}_{kj}^{(p)} = 0 \tag{15}$$

5. HODGE STAR OPERATOR ON A LATTICE

5.1. Interpolants for Discrete Differential Forms

Before proceeding with the transcription of the discrete Hodge star operator to a simplicial lattice, we need first to obtain interpolants of discrete differential forms. Given the value of $\alpha_i^{(p)}$ in (9) associated with the set of all p-simplices that form a lattice, $i = 1, \ldots, N_p$, such interpolants would provide (interpolate) the value of $\alpha^{(p)}$ elsewhere in the ambient spacetime spanned by the lattice. For a 0-form, barycentric coordinates themselves constitute the suitable interpolant, that is

$$\alpha^{(0)}(u) = \sum_i \alpha_i^{(0)} \lambda_i(u), \tag{16}$$

where $\lambda_i(u)$ is simply the value of λ_i at the point u and $\alpha^{(0)}$ is an arbitrary 0-form. From the properties of barycentric coordinates, it is trivial to verify that this interpolation recovers the nodal values (contractions), that is, $\alpha^{(p)}(u = \sigma_{0,i}) = \alpha_i^{(p)}$. Between nodes, the interpolation is linear. As noted before, 0-forms can be associated to *continuous* scalar functions and this interpolation preserves such property.

For differential forms of degree p, we wish to determine suitable interpolants that *generalize the concept of barycentric coordinates from 0-d objects (points) to p-d objects* in such a way that a p-dimensional object can be likewise represented in terms of lattice p-simplices. Note that barycentric

[‡] This constraint generalizes, on the lattice, the identities $\nabla \times \nabla = 0$ and $\nabla \cdot \nabla \times = 0$ of vector calculus to any number of dimensions and distilled from the metric.

coordinates can represent any point u inside, say, a 2-simplex $[u_1,\, u_2,\, u_3]$ in terms of its boundary nodes, that is

$$u = \lambda_1(u)u_1 + \lambda_2(u)u_2 + \lambda_3(u)u_3, \tag{17}$$

which for a 0-form $\alpha^{(0)}$ evaluates as

$$\alpha^{(0)}(u) = \lambda_1(u)\alpha^{(0)}(u_1) + \lambda_2(u)\alpha^{(0)}(u_2) + \lambda_3(u)\alpha^{(0)}(u_3), \tag{18}$$

and recovers (16) for any point u within the 2-simplex $[u_1,\, u_2,\, u_3]$. In (18), we used the fact that for a 0-form the domain of integration $\sigma_{0,i}$ in (9) is simply a point (node), and hence the integration (contraction) reduces to the evaluation of a function (0-form) at such point. This allows us to write $\alpha^{(0)}(u_1) = \alpha_1^{(0)}$ using the notation (9). Furthermore, for reasons that will be clear later on, we denote $\lambda_i = w_i^{(0)}$, $i = 1, 2, 3$ so that (18) can also be written as

$$\alpha^{(0)} = \alpha_1^{(0)} w_1^{(0)} + \alpha_2^{(0)} w_2^{(0)} + \alpha_3^{(0)} w_3^{(0)}. \tag{19}$$

By letting u to be anywhere on the lattice domain, not necessarily restricted to within a given simplex, the above equation generalizes to

$$\alpha^{(0)} = \sum_i \alpha_i^{(0)} w_i^{(0)} \tag{20}$$

where the index i in this sum runs through all nodes of the lattice, $i = 1, \ldots, N_0$. We will next find a suitable generalization of the above equations for p-dimensional objects, representing lines in terms of the edges of the lattice, surfaces in terms of the faces of the lattice, and so on. This generalization was first obtained in [23] and a succinct geometric derivation was provided in [24]. For concreteness, let us examine next the case of a line in 2-d in more detail and from a slightly different perspective here. In Fig. 4, we depict a straight line segment inside a 2-simplex with a point u marked on it. The location of u can be uniquely determined by the value of two of its barycentric coordinates, say λ_1 and λ_2, as indicated. Together with the opposite node u_3, the two end points of this segment, denoted as u_s and u_f comprise an oriented triangle, indicated by the area in red. Assuming that the 2-simplex $[u_1,\, u_2,\, u_3]$ has unit area, it is a simple exercise to show that the area of the triangle $[u_s,\, u_f,\, u_3]$ is equal to $\lambda_1(u_s)\lambda_2(u_f) - \lambda_1(u_f)\lambda_2(u_s)$. This area corresponds to the coefficient of the segment $[u_s,\, u_f]$ expressed in terms of the edge $[u_1,\, u_2]$. Note that this 'area' can assume negative values depending on the relative orientation of the segment versus the edge. By repeating this procedure w.r.t to the other two edges, one can then express the segment $[u_s,\, u_f]$ in terms of the three edges of this 2-simplex as

$$\begin{aligned}[u_s, u_f] = {} & \left(\lambda_1(u_s)\lambda_2(u_f) - \lambda_2(u_s)\lambda_1(u_f)\right)[u_1, u_2] + \left(\lambda_2(u_s)\lambda_3(u_f) - \lambda_3(u_s)\lambda_2(u_f)\right)[u_2, u_3] \\ & + \left(\lambda_3(u_s)\lambda_1(u_f) - \lambda_1(u_s)\lambda_3(u_f)\right)[u_3, u_1].\end{aligned} \tag{21}$$

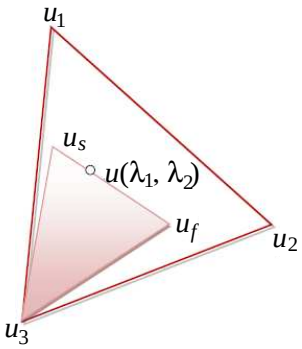

Figure 4. Straight line segment $[u_s,\, u_f]$ within 2-simplex $[u_1,\, u_2,\, u_3]$. Any point along the segment can be uniquely specific by the barycentric coordinates λ_1 and λ_2.

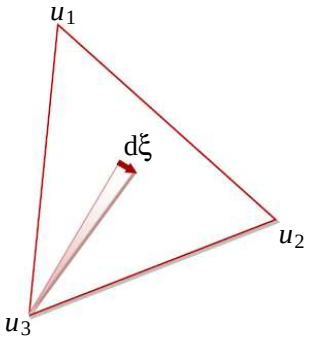

Figure 5. Infinitesimal segment $\mathrm{d}\xi$ within 2-simplex $[u_1,\, u_2,\, u_3]$.

which is the desired generalization of (17) to 1-d objects, where the coefficients in (21) play the role analogous to barycentric coordinates in (17). In order to generalize for the case of non-straight line segments, we consider an oriented infinitesimal segment $\mathrm{d}\xi$ as depicted in Fig. 5. In this case, the two end points of the segment can be expressed in terms of their barycentric coordinates as $(\lambda_1,\, \lambda_2)$ and $(\lambda_1 + \mathrm{d}\lambda_1,\, \lambda_2 + \mathrm{d}\lambda_2)$. They determine the triangle indicated in red in Fig. 5 (with an infinitesimal acute angle). Assuming unit area for the 2-simplex $[u_1,\, u_2,\, u_3]$, it is again easy to show that the infinitesimal area of such triangle is

$$\lambda_1\,(\lambda_2 + \mathrm{d}\lambda_2) - (\lambda_1 + \mathrm{d}\lambda_1)\,\lambda_2 = \lambda_1 \mathrm{d}\lambda_2 - \lambda_2 \mathrm{d}\lambda_1, \tag{22}$$

which represents the coefficient of such differential segment in terms of the edge $[u_1,\, u_2]$. Repeating this procedure for the other two edges and combining, one has

$$\mathrm{d}\xi = (\lambda_1 \mathrm{d}\lambda_2 - \lambda_2 \mathrm{d}\lambda_1)\,[u_1, u_2] + (\lambda_2 \mathrm{d}\lambda_3 - \lambda_3 \mathrm{d}\lambda_2)\,[u_2, u_3] + (\lambda_3 \mathrm{d}\lambda_1 - \lambda_1 \mathrm{d}\lambda_3)\,[u_3, u_1]. \tag{23}$$

Integration of (23) along a path C yields

$$\int_C \mathrm{d}\xi = [u_1, u_2] \int_C (\lambda_1 \mathrm{d}\lambda_2 - \lambda_2 \mathrm{d}\lambda_1) + [u_2, u_3] \int_C (\lambda_2 \mathrm{d}\lambda_3 - \lambda_3 \mathrm{d}\lambda_2) + [u_3, u_1] \int_C (\lambda_3 \mathrm{d}\lambda_1 - \lambda_1 \mathrm{d}\lambda_3)\,. \tag{24}$$

which generalizes (17) from a point to a path. By numbering at this point the edges $[u_1,\, u_2]$, $[u_1,\, u_2]$, $[u_1,\, u_2]$ as 1, 2, and 3 respectively, and using the definitions $(\lambda_1 \mathrm{d}\lambda_2 - \lambda_2 \mathrm{d}\lambda_1) = w_1^{(1)}$, $(\lambda_1 \mathrm{d}\lambda_2 - \lambda_2 \mathrm{d}\lambda_1) = w_2^{(1)}$, and $(\lambda_1 \mathrm{d}\lambda_2 - \lambda_2 \mathrm{d}\lambda_1) = w_3^{(1)}$ then, analogously to the passage (17) from (18), the relation (24) can be applied a 1-form $\alpha^{(1)}$ to yield

$$\int_C \alpha^{(1)} = \alpha_1^{(1)} \int_C w_1^{(1)} + \alpha_2^{(1)} \int_C w_2^{(1)} + \alpha_3^{(1)} \int_C w_3^{(1)}, \tag{25}$$

where we also used the definition in (9). Since (25) is valid for any C, it immediately follows that, within the 2-simplex $[u_1,\, u_2,\, u_3]$, we have

$$\alpha^{(1)} = \alpha_1^{(1)} w_1^{(1)} + \alpha_2^{(1)} w_2^{(1)} + \alpha_3^{(1)} w_3^{(1)}. \tag{26}$$

where it seen that (26) is the 1-form counterpart to the expression for 0-forms obtained in (19). Further, by allowing C to be anywhere on the lattice, and not necessarily within a single 2-simplex $[u_1, u_2, u_3]$, (26) generalizes to

$$\alpha^{(1)} = \sum_i \alpha_i^{(1)} w_i^{(1)} \tag{27}$$

as in (20), where now the index i of this sum runs through all edges of the lattice, $i = 1,\, \ldots,\, N_1$.

For higher dimensional objects, similar expansions can be obtained for differential forms of any degree, that is

$$\alpha^{(p)} = \sum_i \alpha_i^{(p)} w_i^{(p)}. \tag{28}$$

where the sum runs over all faces, volumes or hypervolumes for $p = 2,\, 3,\, 4$ respectively, comprising the lattice. Using steps very analogous to the ones for the $p = 0$ and $p = 1$ cases examined above, the expression for the $w^{(p)}$ interpolant function associated to a p-simplex $\sigma_{p,i} = [u_1, u_2, \ldots, u_{p+1}]$ can be found as [23]

$$w^{(p)}[\sigma_{p,i}] \equiv w_i^{(p)} = (p+1)! \sum_{k=1}^{p+1} (-1)^k \lambda_k \mathrm{d}\lambda_1 \ldots \mathrm{d}\lambda_{k-1} \mathrm{d}\lambda_{k+1} \ldots \mathrm{d}\lambda_{p+1} \tag{29}$$

Collectively, the interpolating functions $w^{(p)}$ are denoted as *Whitney forms*. As noted in [5], it is a simple exercise to verify that

$$\int_{\sigma_{p,j}} w_i^{(p)} = \delta_{ij} \tag{30}$$

with δ_{ij} being the Kronecker delta, and that the following hierarchical construction holds

$$w_i^{(p)}[\sigma_{p,i}] = \mathrm{d}w^{(p-1)}[\partial\sigma_{p,i}]. \tag{31}$$

It should also be stressed that expression (29) is metric-free and therefore invariant regardless of how the p-simplex $\sigma_{p,i}$ is oriented w.r.t. the local spatial and time coordinate axis (metric signature). However, this is *not* true of vector representations (proxies) thereof, which are metric-dependent and hence depend on the relative orientation of the simplicial element w.r.t. to the time axis. In the Riemannian case and using the parlance of finite elements, the vector representations of Whitney 1-forms and 2-forms recover the so-called edge and face vector basis functions respectively, see e.g., [25, 27]. On the other hand, in the Lorentzian case, the vector representation of a Whitney 1-form is exemplified for the $(1+1)$-d Minkowski spacetime in [28].

Whitney forms can be used to expand fields defined on the primal lattice or on the dual lattice. In the former case, (28) can be used directly since the primal lattice is simplicial. In the latter case, (28) can be used first on the (barycentric) decomposition lattice (which is also simplicial as seen before) and a consequent expansion on the dual lattice can be built by assembling elements of the dual lattice from the Whitney elements of the decomposition lattice, as suggested in [13]. A more explicit example of a Whitney complex constructed on barycentric dual lattices is provided in [29].

5.2. Discrete Action and Discrete Hodge Representations

The source-free action from (1) is

$$\mathcal{S} = \frac{1}{2}\int_{\Omega^4} F \wedge G = \frac{1}{2}\int_{\Omega^4} F \wedge *F. \tag{32}$$

Using an expansion for F is terms of Whitney forms, that is

$$F = \sum_i F_i w_i^{(2)}, \tag{33}$$

where the index runs over all the faces of the lattice, the source-free electromagnetic action on the lattice assumes an expected quadratic form in terms of the degrees of freedom of the theory

$$\mathcal{S} = \frac{1}{2}\sum_i \sum_j F_i [*]_{ij}^{(2)} F_j, \tag{34}$$

where we can immediately identify

$$[*]_{ij}^{(2)} = \int_{\Omega^4} \omega_i^{(2)} \wedge *\omega_j^{(2)} \tag{35}$$

as a discrete realization of the Hodge star operator [6, 25] on a 4-d simplicial lattice with Minkowski spacetime background. Note that, from (32) and (35), one can equivalently write

$$G_i = \sum_j [*]_{ij}^{(2)} F_j \tag{36}$$

so that the source-free action on the lattice can be also expressed as

$$\mathcal{S} = \frac{1}{2}\sum_i E_i G_i \tag{37}$$

where again the index runs over all the faces of the lattice.

5.3. Hodge and Poincaré Dualities

Equation (36) establishes a Hodge duality between the DoFs of $F = *G$ at the discrete level. As noted before, this duality also establishes a connection between primal and dual lattice quantities. Even without reference to a field theory, a notion of duality is already present because of the bijective correspondence between p-simplices of the primal lattice and $(n-p)$-cells of the dual lattice, as formalized by the Poincaré duality theorem [26].

6. LATTICE FIELD EQUATIONS

6.1. 4-d Theory

Application of the counterpart of (11) in the dual lattice to the relation $\mathrm{d}G = *\mathcal{J}$ yields

$$\int_{\tilde{\sigma}_{3,i}} \mathrm{d}G = \sum_j \tilde{C}^{(3)}_{ij} \int_{\tilde{\sigma}_{2,j}} G = \int_{\tilde{\sigma}_{3,i}} (*\mathcal{J}) \tag{38}$$

for all 3-cells i on the dual lattice. By using again the shorthand notation introduced (9) and the discrete Hodge duality (36), one obtains

$$\sum_j \tilde{C}^{(3)}_{ij} \left(\sum_k [*]^{(2)}_{jk} F_k \right) = (*\mathcal{J})_i \tag{39}$$

Similarly, application of (11) to $\mathrm{d}F = 0$ yields the constraint

$$\sum_i C^{(3)}_{ij} F_j = 0 \tag{40}$$

for all 3-simplices i on the primal lattice. From $F = \mathrm{d}A$, one has

$$F_i = \sum_j C^{(2)}_{ij} A_j \tag{41}$$

and hence $\mathrm{d}F = 0$ holds exactly from (14). In addition, (39) becomes

$$\sum_j \tilde{C}^{(3)}_{ij} \left[\sum_k [*]^{(2)}_{jk} \left(\sum_l C^{(2)}_{kl} A_l \right) \right] = (*\mathcal{J})_i \tag{42}$$

Again, this equation is verified for all 3-cells $\tilde{\sigma}_{3,i}$ of the dual lattice. As noted before, the DoFs of the potential A are associated with edges (1-simplices) $\sigma_{1,i}$ of the primal lattice, which are in $1:1$ pairing with $\tilde{\sigma}_{3,i}$.

Either (39) together with constraint (40), or (42) can be utilized to solve for the degrees of freedom of the lattice theory. Some important observation are in order. First, at this level of description, we have a boundary value problem in the flat Minkowski 4-d spacetime where time and spatial variable are in an equal setting. The main difficulty associated with such 4-d spacetime formulation is that the Minkowski metric is indefinite (Lorentzian manifold). As a result, the discrete Hodge star operator in (35) and conspicuously present on (39) and (42) corresponds to an indefinite matrix. In particular, if proper care is not exercised in the construction of the 4-d spacetime lattice, many elements with (near) zero measure may ensue. This can cause numerical problems related to division by zero and also makes it difficult to enforce causality constraints, as discussed below. Indeed, the coordination number in a indefinite-metric lattice (i.e., number of lattice 0-simplices within some small distance from any given reference 0-simplex) can be very large and increases with the number of lattice elements, since it will include all 0-simplices within a small distance from the light-cone defined by the reference 0-simplex. This feature is in sharp contrast to the case of a positive-definite metric (Riemannian manifold), which yields a small coordination number. In a number of contexts, a Wick rotation is performed to alleviate the difficulties associated with an indefinite metric [3, 30, 31]. The Wick rotation corresponds to an analytical continuation to imaginary time, $t \to i\tau$ to transform the Lorentzian metric $\mathrm{d}s^2 = \mathrm{d}x^s + \mathrm{d}y^2 + \mathrm{d}z^2 - (c\mathrm{d}t)^2$ into a positive metric in a 4-d Euclidean space $\mathrm{d}s^2 = \mathrm{d}x^2 + \mathrm{d}y^2 + \mathrm{d}z^2 + (ic\,\mathrm{d}\tau)^2$. However, for this procedure to be useful in the present context, one needs to analytically continue back to real time. This becomes difficult to achieve on numerical (not analytical) results. Also, a Wick rotation does not necessarily facilitate causality preservation on the 4-d lattice.

6.2. Causality Constraints on the 4-d Lattice Structure

Causality conditions put constraints on the spacetime mesh that are even stronger than simply avoiding elements with (near) zero measure. Such constraints have been examined before in the context of "causal

dynamic triangulations" [32, 33], for example. In short, they require not only that any edge should be either space-like (positive length) or time-like (negative length), but also that subsets of spatial edges should comprise Cauchy "surfaces" (volumes in 4-d) with positive definite metric in such a way that the 4-d spacetime lattice can be generated from an extrusion of such Cauchy "surfaces" along the time direction. The resulting 4-d lattice in this case has a layered structure with a well-defined causality cone ("light-cone") at every node. Together, the set of such causality cones comprise a globally-consistent set where non-causal features such as closed loops consisting of time-like edges do not occur.

A layered lattice structure can be relaxed by employing so-called "locally-causal dynamical triangulations" where more general connectivity rules between space-like and time-like edges are employed to effect a well-defined causal cone at every lattice node. In short, this is achieved by making sure that, at every node, there are two and only two "opposite" directions containing time-like edges and separated by a region containing only space-like edges [34]. This is illustrated in Fig. 6. Other approaches to construct causality-preserving spacetime lattices also exist, based on generalized advancing-front algorithms. These are discussed in detail in [35, 36].

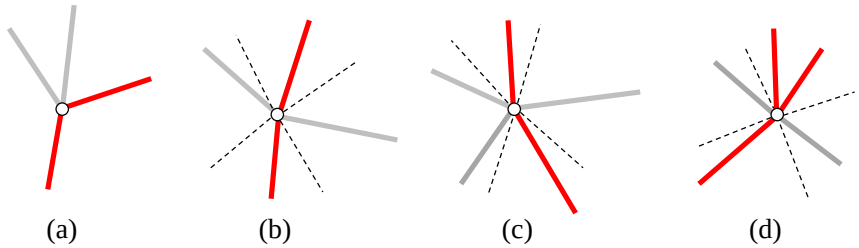

Figure 6. Node-to-edge connectivity examples on a spacetime lattice. Red segments indicate time-like edges and gray segments indicated space-like edges. A simple 2-d arrangement is displayed for visualization purposes, but the same basic rules apply in 4-d. A connectivity such as (a) is not compatible with causality since it does not support two separate light cones emanating from the node (i.e., the definition of a past-to-future chronology is not possible on that node). Cases (b), (c), and (d) are permissible since two non-overlapping light cones can be well-defined, as indicated by the dashed lines. Of course, this is only a necessary condition since all light cones need also to be globally coordinated across nodes.

6.3. (3 + 1)-d Theory

In many practical applications, relativistic effects are not important and it is more convenient to, instead of considering the more general 4-d problem, consider the $(3+1)$-d initial-boundary value problem of determining the time evolution of the fields across spatial slices of fixed geometry. In such $3+1$ setting, one can decompose the F and G 2-forms as [9, 37]

$$F = E\mathrm{d}t + B \tag{43}$$

$$G = D - H\mathrm{d}t \tag{44}$$

and the current-source density as

$$*\mathcal{J} = -J\mathrm{d}t + \rho \tag{45}$$

where E and H are the electric intensity and magnetic intensity 1-forms; D and B are the electric flux and magnetic flux 2-forms; J is the electric current density 2-form; ρ is the electric charge density 3-form [6]. The decomposition (43) is illustrated in Fig. 7. Substituting (43), (44), and (45) in (3) and (4), we obtain

$$\mathrm{d}_s H = \frac{\partial}{\partial t} D + J \tag{46}$$

$$\mathrm{d}_s E = -\frac{\partial}{\partial t} B \tag{47}$$

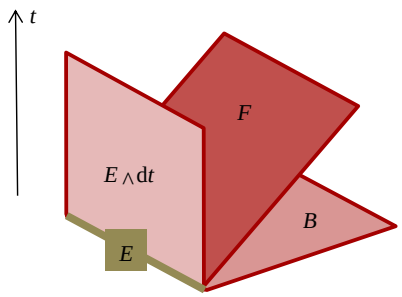

Figure 7. Representation of the Faraday 2-form F, the associated 2-form $E\mathrm{d}t$ oriented parallel to the time axis, and the 2-form B located within the spatial slice. As indicated, the "projection" of $E\mathrm{d}t$ onto the spatial slice corresponds to the 1-form E. For the purposes of visualization, the 3-d spatial slice is represented as 2-d instead. These two "projections" can be utilized once the 4-d lattice elements are properly aligned w.r.t. the time and spatial-slice directions.

supplemented by the constitutive relations $D = \star_\epsilon E$ and $H = \star_{\mu^{-1}} B$ now involving two Hodge star operators in 3-d space. In the above, d_s stands for the 3-d spatial exterior derivative related to the 4-d spacetime exterior derivative through

$$\mathrm{d}(\cdot) = \mathrm{d}_s(\cdot) + \frac{\partial}{\partial t}(\cdot)\mathrm{d}t \tag{48}$$

Note that both (47) and (46) are metric-free. The subscripts ϵ and μ attached to $\star_\epsilon$ and $\star_{\mu^{-1}}$ indicate that these operators can also incorporate background material properties (we assume dispersionless media for simplicity).

In this case, the 4-d lattice can be simply created from an extrusion, along the time coordinate, of the 3-d lattice representing the (fixed) spatial-slice geometry. One can then either "degeometrize" time [5, 6] and treat t simply as a parameter along the direction of extrusion or define generalized Whitney forms on the prismatic elements of the resulting spacetime lattice. These two choices will be considered separately next.

6.3.1. $(3+1)$-d Theory with Degeometrized Time

In the first scenario, using Whitney forms on the 3-d spatial lattice, we can write the following expansions

$$E(t,\nu) = \sum_i E_i(t)\omega_i^{(1)}(\nu) \tag{49}$$

$$B(t,\nu) = \sum_i B_i(t)\omega_i^{(2)}(\nu) \tag{50}$$

where ν represents a generic point within the 3-d spatial slice, and the indices i run over all primal lattice edges and faces for E and B, respectively. In source-free media, the electromagnetic Hamiltonian is [6]

$$\mathcal{H} = \int_{\Omega_3} \left(E \wedge \star_\epsilon E + \star_{\mu^{-1}} B \wedge B\right) \tag{51}$$

Using (49) and (50), the Hamiltonian on a lattice becomes

$$\mathcal{H} = \sum_i \sum_j E_i(t)[\star_\epsilon]_{ij}^{(1)} E_j(t) + \sum_i \sum_j B_i(t)[\star_{\mu^{-1}}]_{ij}^{(2)} B_j(t) \tag{52}$$

where the two symmetric positive definite matrices

$$[\star_\epsilon]_{ij}^{(1)} = \int_{\Omega_3} \omega_i^{(1)}(\nu) \wedge \star_\epsilon \omega_j^{(1)}(\nu) \tag{53}$$

$$[\star_{\mu^{-1}}]_{ij}^{(2)} = \int_{\Omega_3} \left(\star_{\mu^{-1}} \omega_i^{(2)}(\nu)\right) \wedge \omega_j^{(2)}(\nu) \tag{54}$$

correspond to the discretization of $\star_\epsilon$ and $\star_{\mu^{-1}}$, respectively [5, 38, 39]. The indices in (53) and (54) run over the edges and faces of the (spatial-slice) primal lattice, respectively. Discretization of (46) and (47) follows the same basic tenets discussed before in the 4-d case and leads to [5, 6, 25]

$$-\frac{\partial}{\partial t}B_i(t) = \sum_j C_{ij}^{(s,1)}\, E_j(t) \tag{55}$$

where the index i runs over all faces of the primal lattice and

$$\sum_j [\star_\epsilon]_{ij}^{(1)}\, \frac{\partial}{\partial t}E_j(t) = \sum_j C_{ji}^{(s,1)} \sum_k [\star_{\mu^{-1}}]_{jk}^{(2)} B_k(t) \tag{56}$$

where the index i runs over all faces of the dual lattice. The superscript s is used on the (spatial-slice) incidence operators in (55) and (56) to distinguish them from the incidence operators defined previously in (10) for the 4-d spacetime lattice. We stress again that in the expansions (49) and (50) time is fully degeometrized and a number of different time-discretization schemes can be subsequently used for the semi-discrete equations (55) and (56).

6.3.2. Geometric $(3+1)$*-d Theory*

Alternatively, one can still treat the time variable from a geometrical standpoint by defining *prismatic* cells in 4-d, with cross-sections within the spatial slices comprised by the volume simplices of the spatial 3-d lattice. Recall that A is a 1-form in 4-d spacetime. Consequently,

$$A = \sum_i A_i\, w_i^{(1)}, \tag{57}$$

where the sum runs over the spacetime lattice edges. Similar to (43) and (44), one can decompose A in the $(3+1)$-d case as [9]

$$A = A_\nu - \phi \mathrm{d}t \tag{58}$$

where the spatial component A_ν corresponds to the magnetic vector potential and ϕ to the electric scalar potential. Similarly, expansion (57) can be likewise decomposed in $(3+1)$-d as

$$A(\nu, t) = \sum_n \left(\sum_i A_{\nu,i}^n \tau_n(t)\, w_i^{(1)}(\nu) - \sum_i \phi_i^n \pi_n(t) w_i^{(0)}(\nu) \mathrm{d}t \right), \tag{59}$$

where the index i now runs over all edges and nodes of the (simplicial) 3-d lattice comprising the spatial slice. The functions $\tau_n(t)$ and $\pi_n(t)$ are pulse-shaped and triangular-shaped functions, respectively, as illustrated in Fig. 8, and the index n enumerates successive discrete time instants. The factors $\tau_n(t)$ and $\pi_i^n(t)dt$ correspond to Whitney 0- and 1-forms in 1-d (i.e., along temporal direction), respectively. Next, by using $F = \mathrm{d}A$ and (43), the resulting expansions for E and B become

$$E(t, \nu) = \sum_n \sum_i E_i^n \pi_n(t) \omega_i^{(1)}(\nu) \tag{60}$$

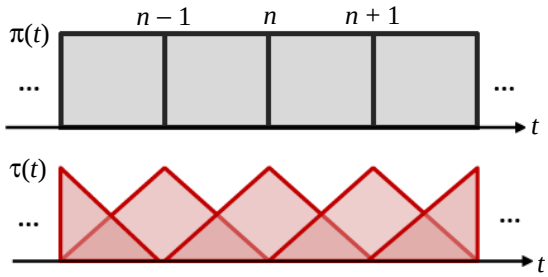

Figure 8. Time-dependent factors $\pi_n(t)$ and $\tau_n(t)$ used in the expansion of the four-vector potential $A(\nu, t)$.

$$B(t,\nu) = \sum_n \sum_i B_i^n \tau_n(t) \omega_i^{(2)}(\nu) \tag{61}$$

where $\pi_n(t)\omega_i^{(1)}(\nu)$ and $\tau_n(t)\omega_i^{(2)}(\nu)$ can be recognized as "generalized" Whitney forms associated with the prismatic elements of such (extruded) spacetime lattice.

The reason for the different expansions w.r.t. the time variable in E and B can be traced down to (43), where it is seen that E is associated with the temporal components of the 4-d exterior derivative (48). Consequently, the degree of continuity of E along the time direction is one less than that of B. This can also be seen directly from (47). Note also that, as depicted in Fig. 8, the midpoints along t of $\pi_n(t)$ and $\tau_n(t)$ do not coincide: $\tau_n(t)$ is centered at integer indices whereas $\pi_n(t)$ is centered at half-integer indices. Such staggering of the E and B field expansions in time makes the above expansions compatible with (47). In the context of numerical methods such as the finite-difference time-domain (FDTD) [40–42], it provides a fundamental justification for the use of staggered discretizations such as leap-frog time integration.

7. CONCLUSIONS

We described a lattice formulation for 4-d Maxwell's equations based on the representation of field and causative source quantities as differential forms of various degrees. The degrees of freedom of the theory are localized on specific types of lattice elements according to the kind of differential form they are associated with. Primal and dual lattices are employed to accommodate the need to represent field quantities with different types of orientation (inner and outer). Whitney forms are used to construct discrete Hodge operators and define an isomorphism between the primal lattice and the barycentric dual lattice. Lattice field theories in $(3+1)$-d are considered as special cases of the 4-d theory following a specific choice of alignment for the lattice elements.

ACKNOWLEDGMENT

This work was supported in part by NSF under grant ECCS-1305838. Some portions of this paper have appeared before in [6].

REFERENCES

1. Bott, R., "On some recent interactions between mathematics and physics," *Canad. Math. Bull.*, Vol. 28, No. 2, 129–164, 1985.
2. Göckeler, M. and T. Schüker, *Differential Geometry, Gauge Theories, and Gravity*, Cambridge University Press, 1987.
3. Burgess, M., *Classical Covariant Fields*, Cambridge University Press, 2002.
4. Zee, A., *Quantum Field Theory in a Nutshell,* Princeton University Press, Princeton, NJ, 2003.
5. Teixeira, F. L. and W. C. Chew, "Lattice electromagnetic theory from a topological viewpoint," *J. Math. Phys.*, Vol. 40, No. 1, 169–187, 1999.
6. Teixeira, F. L., "Differential forms in lattice field theories: An overview," *ISRN Math. Phys.*, Vol. 2013, 487270, 2013.
7. Tarhasaari, T., L. Kettunen, and A. Bossavit, "Some realizations of a discrete Hodge operator: A reinterpretation of finite element techniques," *IEEE Trans. Magn.*, Vol. 35, No. 3, 1494–1497, 1999.
8. Misner, C. W., K. S. Thorne, and J. A. Wheeler, *Gravitation,* Freeman and Co., New York, 1973.
9. Deschamps, G. A., "Electromagnetics and differential forms," *Proc. IEEE*, Vol. 69, 676–696, 1982.
10. Schenberg, M., "Electromagnetism and gravitation," *Braz. J. Phys.*, Vol. 1, 91–122, 1971.
11. Warnick, K. F. and P. Russer, "Two, three, and four-dimensional electromagnetics using differential forms," *Turk. J. Elec. Engin.*, Vol. 14, No. 1, 153–172, 2006.
12. Gross, P. W. and P. R. Kotiuga, "Data structures for geometric and topological aspects of finite element algorithms," *Progress In Electromagnetics Research*, Vol. 32, 151–169, 2001.

13. Teixeira, F. L., "Geometrical aspects of the simplicial discretization of Maxwell's equations," *Progress In Electromagnetics Research*, Vol. 32, 171–188, 2001.
14. Tonti, E., "Finite formulation of the electromagnetic field," *Progress In Electromagnetics Research*, Vol. 32, 1–44, 2001.
15. Gross, P. W. and P. R. Kotiuga, *Electromagnetic Theory and Computation: A Topological Approach*, Cambridge University Press, 2004.
16. Adams, D. H., "R-torsion and linking numbers from simplicial Abelian gauge theories," *High Energy Physics — Theory*, 9612009, 1996.
17. Sen, S., S. Sen, J. C. Sexton, and D. H. Adams, "Geometric discretization scheme applied to the Abelian Chern-Simons theory," *Phys. Rev. E*, Vol. 61, No. 3, 3174–3185, 2000.
18. Clemens, M. and T. Weiland, "Discrete electromagnetism with the finite integration technique," *Progress In Electromagnetics Research*, Vol. 32, 65–87, 2001.
19. Schuhmann, R. and T. Weiland, "Conservation of discrete energy and related laws in the finite integration technique," *Progress In Electromagnetics Research*, Vol. 32, 301–316, 2001.
20. He, B. and F. L. Teixeira, "On the degrees of freedom of lattice electrodynamics," *Phys. Lett. A*, Vol. 336, No. 1, 1–7, 2005.
21. Kheyfets, A. and W. A. Miller, "The boundary of a boundary in field theories and the issue of austerity of the laws of physics," *J. Math. Phys.*, Vol. 32, No. 11, 3168–3175, 1991.
22. Guth, A. H., "Existence proof of a nonconfining phase in four-dimensional U(1) lattice field theory," *Physical Review D*, Vol. 21, No. 8, 2291–2307, 1980.
23. Whitney, H., *Geometric Integration Theory,* Princeton University Press, Princeton, NJ, 1957.
24. Bossavit, A., "'Generalized finite differences' in computational electromagnetics," *Progress In Electromagnetics Research*, Vol. 32, 45–64, 2001.
25. He, B. and F. L. Teixeira, "Geometric finite element discretization of Maxwell equations in primal and dual spaces," *Phys. Lett. A*, Vol. 349, Nos. 1–4, 1–14, 2006.
26. Schwarz, A. S., *Topology for Physicists,* Springer-Verlag, New York, 1994.
27. Bossavit, A., "Whitney forms: A new class of finite elements for three-dimensional computations in electromagnetics," *IEE Proc. A*, Vol. 135, 493–500, 1988.
28. Salamon, J., J. Moody, and M. Leok, "Geometric representations of Whitney forms and their generalization to Minkowski spacetime," *Numerical Analysis*, 1402.7109, 2014.
29. Buffa, A. and S. Christiansen, "A dual finite element complex on the barycentric refinement," *Math. Comput.*, Vol. 76, 1743–1769, 2007.
30. Osterwalder, K. and R. Schrader, "Axioms for Euclidean Green's functions," *Comm. Math. Phys.*, Vol. 31, No. 2, 83–112, 1973.
31. Montvay, I. and G. Munster, *Quantum Fields on a Lattice*, Cambridge University Press, 1994.
32. Ambjorn, J., J. Jurkiewicks, and R. Loll, "Emergence of a 4D world from causal quantum gravity," *Phys. Rev. Lett.*, Vol. 93, 131301, 2004.
33. Ambjorn, J., A. Gorlich, J. Jurkiewicks, and R. Loll, "Nonperturbative quantum gravity," *Phys. Rep.*, Vol. 519, 127, 2012.
34. Jordan, S. and R. Loll, "Causal dynamical triangulations without preferred foliation," *High Energy Physics — Theory*, 1305.4582, 2013.
35. Erickon, J., D. Guoy, J. M. Sullivan, and A. Ungor, "Buliding space-time meshes over arbitrary spatial domains," *Engg. Computers*, Vol. 290, 342–353, 2005.
36. Thite, S., "Adaptive spacetime meshing fod discontinuous Galerkin methods," *Comp. Geom.*, Vol. 42, No. 1, 20–44, 2009.
37. Stern, A., Y. Tong, M. Desbrun, and J. E. Mardsen, "Variational integrators for mMxwell's equations with sources," *PIERS Online*, Vol. 4, No. 7, 711–715, 2008.
38. Kim, J. and F. L. Teixeira, "Parallel and explicit finite-element time-domain method for Maxwell's equations," *IEEE Trans. Antennas Propagat.*, Vol. 59, No. 6, 2350–2356, 2011.

39. Tarhasaari, T., L. Kettunen, and A. Bossavit, "Some realizations of the discrete Hodge operator: A reinterpretation of finite element techniques," *IEEE Trans. Magn.*, Vol. 35, No. 3, 1494–1497, 1999.
40. Yee, K. S., "Numerical solution of initial boundary value problems involving Maxwell's equation is isotropic media," *IEEE Trans. Antennas Propagat.*, Vol. 14, No. 3, 302–307, 1969.
41. Taflove, A., *Computational Electrodynamics: The Finite-difference Time-domain Method,* Artech House, Norwood, MA, 1995.
42. Mattiussi, C., "The geometry of time-stepping," *Progress In Electromagnetics Research*, Vol. 32, 123–149, 2001.